

## Three-axis MEMS Accelerometer for Structural Inspection

E Barbin<sup>1</sup>, A Koleda<sup>1</sup>, T Nesterenko<sup>2</sup>, S Vtorushin<sup>3</sup>

<sup>1</sup>Engineer, Tomsk Polytechnic University, Tomsk, Russia

<sup>2</sup>Associate professor, Tomsk Polytechnic University, Tomsk, Russia

<sup>3</sup>Ph.d. student, Tomsk Polytechnic University, Tomsk, Russia

E-mail: bar\_es@mail.ru

**Abstract.** Microelectromechanical system accelerometers are widely used for metrological measurements of acceleration, tilt, vibration, and shock in moving objects. The paper presents the analysis of MEMS accelerometer that can be used for the structural inspection. ANSYS Multiphysics platform is used to simulate the behavior of MEMS accelerometer by employing a finite element model and MATLAB/Simulink tools for modeling nonlinear dynamic systems.

### 1. Introduction

The modern instrumentation engineering opens new vistas for the development of low-weight and small-size devices of low cost, energy consumption, and high reliability. Microelectromechanical systems (MEMS) comply with these properties due to their micron size, advanced functionality, low energy consumption and cost, and mass-scale application. Nowadays, the MEMS market rapidly grows: the annual increase of the market demand comes to 14–20 % as shown in figure 1 [1].

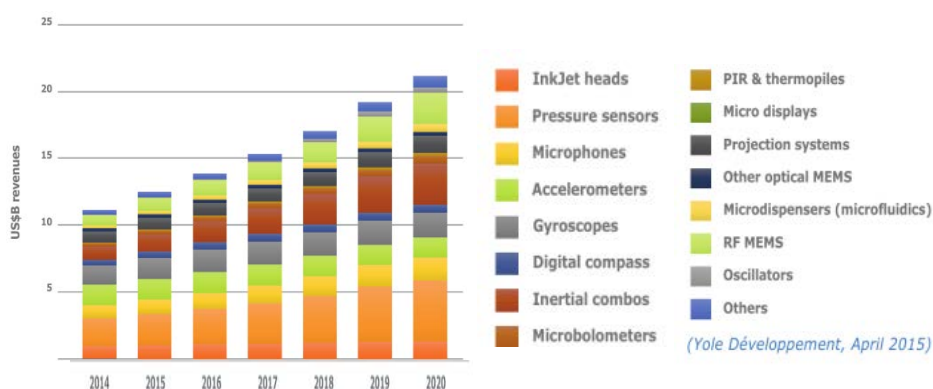


Figure 1. MEMS market forecast.

The increase of the buildings service life as well as the improvement of occupational safety conditions is the worldwide tendency of today. The development of safety systems and continuous monitoring of buildings, bridges, railways is very important to achieve these purposes. MEMS seismic sensors are used in the capacity of railway safety systems. Conventional patrolling is being replaced by the intelligent inspection systems. If somebody tries to do a mine hole under a railroad bed, the alarm is generated on the operator's desk [2].

In connection with the new national standard of the structural inspection accepted in Russia in 2011, it is necessary to perform the building construction monitoring. This becomes possible with the



use of the wireless sensor network (WSN) that allows inspecting such characteristics as vibration, deformation, deviation, etc. with the periodicity convenient for a user. A wireless sensor network consists of spatially distributed autonomous sensor nodes and execution units unified by a radio channel to monitor physical or/and environmental conditions. WSN coverage area can achieve several kilometers due to the messages forwarding from one element to another. The monitoring system includes different types of sensors installed on structural elements of a building with a view to detect both the physical (humidity and temperature) and force (static and dynamic loads) effects on their strength and deformation properties [3]. Therefore, the market of building construction monitoring is rather a promising direction of the WSN implementation in Russia. Moreover, the appropriate control for the execution of diagnosis and industrial safety acts affects the WSN market that can be estimated at billions of dollars [2].

## 2. Description and architecture of accelerometer

A microelectromechanical system accelerometer is one of the wireless sensors both embedded in inclinometer (an instrument for measuring angles of borehole, elevation or depression of an object with respect to the Earth's gravitational field and independent 1-, 2-, and 3-axis units intended for measuring vibrations along the selected axes of an object).

The purpose of this work is to design a three-axis MEMS accelerometer. The function scheme of this accelerometer sensor is shown in figure 2. The frame 3 is mounted on the bottom silicon wafer 12 by the elastic suspension 9 and anchors 10. Sensor is covered with the top silicon wafer 11. Planar electrodes 15, 16 are sprayed on top and bottom silicon wafers. The elastic suspension provides the frame movement along Z axis together with the moving masses 1, 6 moving along X and Y axes, respectively.

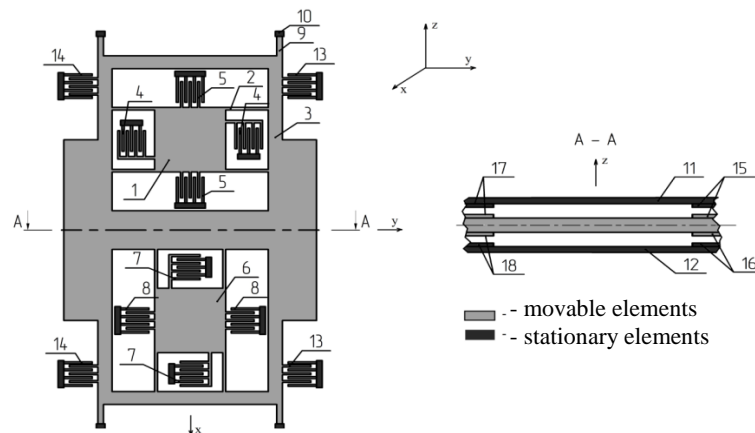


**Figure 2.** Function scheme of accelerometer sensor: 1, 6 – moving masses; 2, 9 – elastic suspension; 3 – frame; 4, 5, 7, 8, 13, 14 – comb electrodes; 10 – anchor; 11 – top silicon wafer, 12 – bottom silicon wafer; 15, 16, 17, 18 – planar electrodes.

Comb electrodes 4 are incorporated into the mechanical movement transducer of the moving mass 1 along X axis. This mechanical movement occurs due to the acceleration along X axis. Comb electrodes 5 serve as the execution units that form the correction forces and compensating feedback in X-direction. Comb electrodes 7 are incorporated into the mechanical movement transducer of the moving mass 6 along Y axis. This mechanical movement occurs due to the acceleration along Y axis. Comb electrodes 8 serve as the execution units that form the correction forces and compensating feedback in Y-direction. Planar electrodes 15, 16, 17, 18 are incorporated into the mechanical movement transducer to detect the motion of frame 3 along Z axis. This mechanical movement occurs in case of the acceleration along Z axis. Comb electrodes 13, 14 serve as the execution units that form the correction forces and compensating feedback in Z-direction.

Let us generate the equation for the movement of the accelerometer sensor the equivalent scheme of which is presented in figure 3. It is assumed that stiffness  $G_z, G_x, G_y$  of elastic suspensions is much lesser on the sensor sensitive axes than that of the same suspensions in crossing directions. This assumption is ground and very important for the design of accelerometer sensor. Sensor coordinates  $OXYZ$  shown in figure 4 are associated with the frame which performs a translational motion with the acceleration having  $XYZ$ -components, namely  $a_x, a_y, a_z$  and rotates with  $\Omega_x, \Omega_y, \Omega_z$  angular velocities. Coordinates  $O_1X_1Y_1Z_1$  are connected with the moving mass 1, coordinates  $O_2X_2Y_2Z_2$  – with the moving mass 2, while coordinates  $O_3X_3Y_3Z_3$  are connected with the frame.

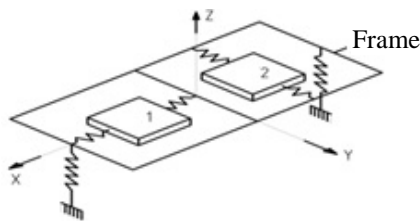


**Figure 3.** Equivalent scheme of accelerometer sensor.

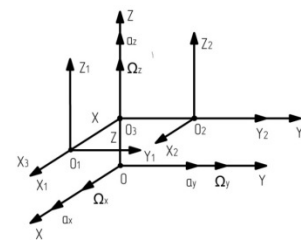


**Figure 4.** Sensor coordinates.

The motion equations for the accelerometer sensor can be obtained from Lagrange equations of the second order:

$$\begin{aligned} & (m_1 + m_2 + m_3)\ddot{z} + z[G_z - (m_1 + m_2 + m_3)(\Omega_y^2 + \Omega_x^2)] + \mu_z\dot{z} = \\ & = (m_1 + m_2 + m_3)a_z - 2m_2\Omega_x\dot{y} + 2m_1\Omega_y\dot{x} - m_2y \cdot \Omega_z\Omega_y - m_1x\Omega_x\Omega_z \\ & m_1\ddot{x} + \mu_x\dot{x} + x[G_x - m_1(\Omega_z^2 + \Omega_y^2)] = m_1a_x - 2m_1\Omega_y\dot{z} + m_1z\Omega_x\Omega_z \\ & m_2\ddot{y} + \mu_y\dot{y} + y[G_y - m_2(\Omega_x^2 + \Omega_z^2)] = m_2a_y + 2m_2\Omega_x\dot{z} - m_2z\Omega_y\Omega_z, \end{aligned}$$

where  $m_1, m_2, m_3$  are masses of bodies 1, 5 and 4 respectively;  $G_z, G_x, G_y$  are stiffness coefficients of suspensions;  $\mu_x, \mu_y, \mu_z$  are the coefficients of viscous friction force in the direction of the respective generalized coordinates;  $a_x, a_y, a_z$  are accelerations of the translational motion of the object.

### 3. Research and results

Eigenfrequencies and eigenmodes of the accelerometer are presented in figure 5. Its behavior is simulated using the ANSYS Multiphysics platform. The geometry of MEMS accelerometer is designed such that the eigenfrequencies are close to each other along all three axes.

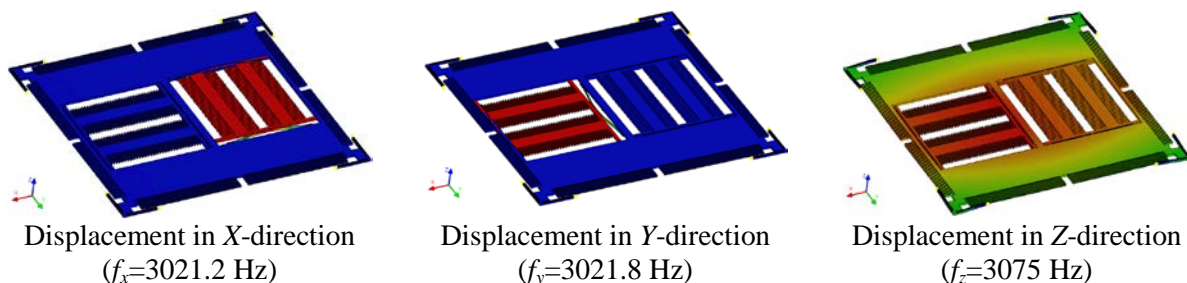


**Figure 5.** Eigenfrequencies and eigenmodes of MEMS accelerometer.

The modal analysis allows obtaining the coefficients of stiffness along the respective axes:

$$G_i = \frac{m_i}{\omega_i^2}.$$

MEMS accelerometers should operate at the temperature range of  $-40^{\circ}\text{C}$  to  $85^{\circ}\text{C}$  guaranteeing their functional properties. The internal stresses occurred due to the extension of the sensor structure is the main factor that affects eigenfrequencies. The temperature effect induces structural changes in geometry, Young's modulus of silicon and, thereby, internal stresses [4–6].

The temperature effect is investigated within the range from  $-40^{\circ}\text{C}$  to  $105^{\circ}\text{C}$ . A change of eigenfrequencies results in a change of the mechanical scale factor of accelerometer sensor. Figures 6 and 7 contain the plots of the temperature dependencies for eigenfrequencies and the scale factor.

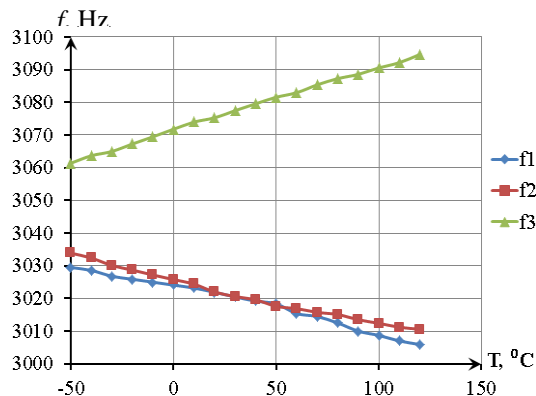


**Figure 6.** Eigenfrequencies vs. temperature.

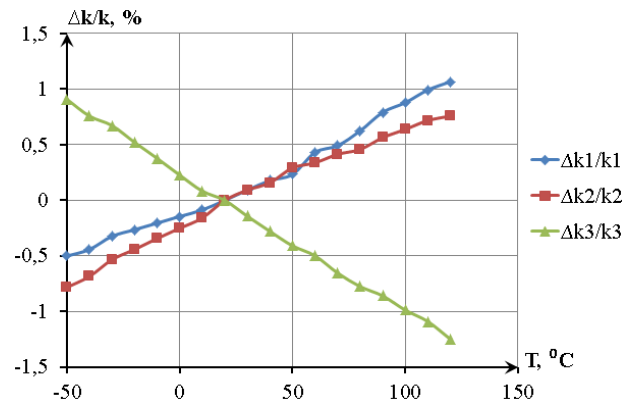


**Figure 7.** Scale factor vs. temperature.

The temperature effect on the accelerometer geometry modifies the capacitance of electrode structures, and an error is introduced in the output signal of the sensor. The accelerometer capacitances are presented in figure 8. The range of motion of the movable sensor element is  $\pm 1 \mu\text{m}$ . The meshes generated using the finite element method (FEM) for the dependencies between capacitances of the comb structure and the temperature are presented in figure 9.

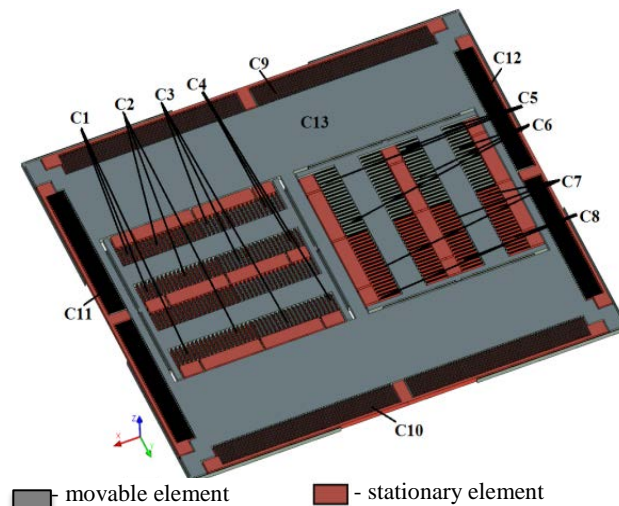


**Figure 8.** Sensor capacitances.

Thus, the maximum change in scale factors of the accelerometer sensor due to temperature changes within the selected temperature range is less than 1%. Errors produced by changes in capacitances of comb structures are not over 2%. Methods of compensation of temperature errors are described in works [4–6].

The results of the modal, thermal, and electrostatic analyses allow the design of the system model of accelerometer shown in figure 10.

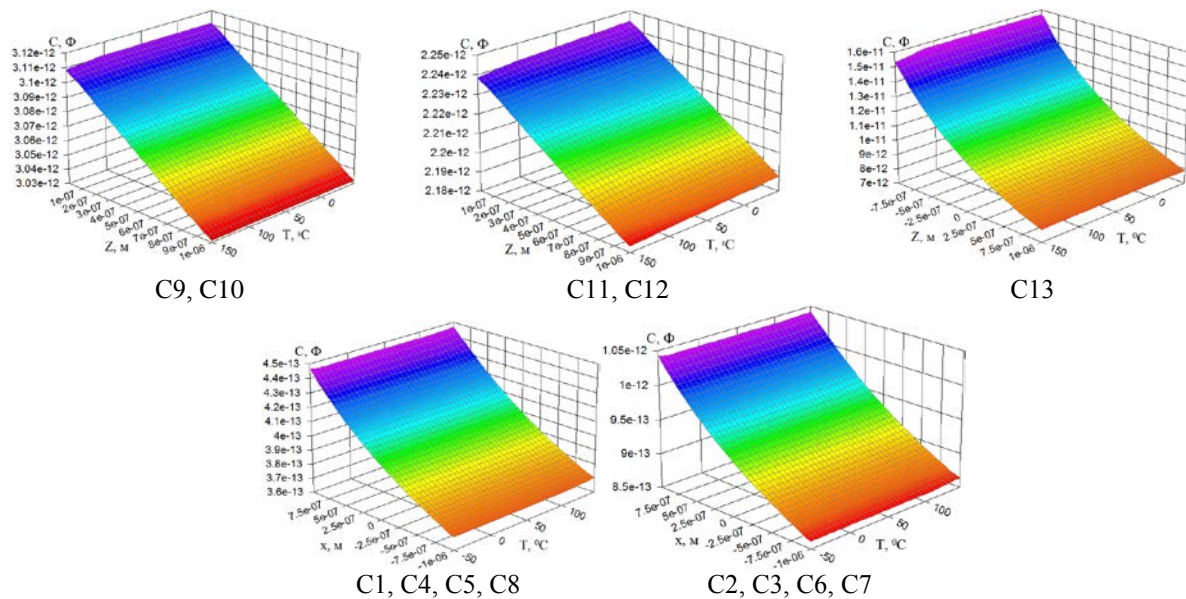


**Figure 9.** Dependences between comb structure capacitances and temperature. Motion range  $\pm 1 \mu\text{m}$ .

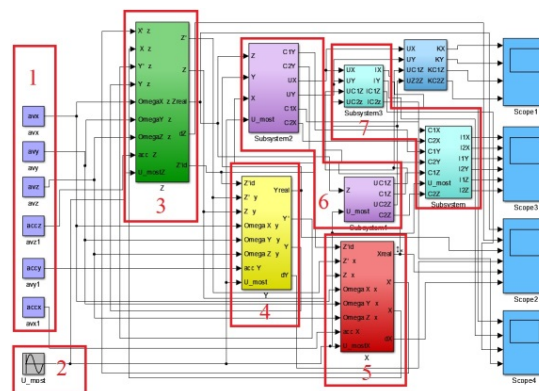


**Figure 10.** Layout of microaccelerometer modeled using MATLAB/Simulink software:  
 1 – sources of disturbance; 2 – the source of voltage for data retrieval form measuring bridge;  
 3 – acceleration measurement channel on the X-axis; 4 – acceleration measurement channel on the Y-axis; 5 - acceleration measurement channel on the Z-axis; 6 – subsystem of measuring bridge;  
 7 – subsystem for calculation of output currents.

The elastic force vector is calculated at each time interval. This model has been developed in several stages, beginning from separate parts to the whole system and including modeling of the ideal system. Figure 11 contains a plot of the dependence between the output voltage and acceleration, and figure 12 describes the motion of frames at sinusoidal behavior of acceleration.

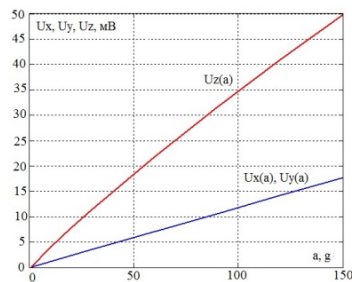


**Figure 11.** Output voltage/acceleration dependence.

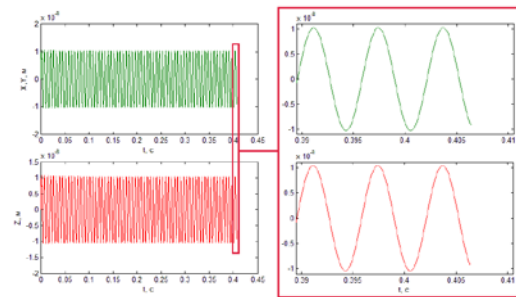


**Figure 12.** Frame motion at sinusoidal behavior of acceleration.

Cross-coupling errors are then modeled subject to angular velocities  $\Omega_y$ ,  $\Omega_x$ ,  $\Omega_z$ , and the output signal error is determined. The dependence between the variability of the cross-coupling error and angular velocities is given in figure 13.

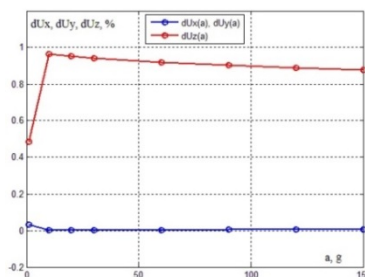


**Figure 13.** Cross-coupling error and angular velocity dependence on X and Y axes.

#### 4. Conclusion

As a result of this research, the three-axis MEMS accelerometer was designed. It can be applied in the field of building construction monitoring.

#### Acknowledgements

The authors acknowledge the financial support from the Ministry of Education and Science of the Russian Federation (agreement N 14.575.21.0068, unique identifier RFMEFI57514X0068) of this research that was carried out at Tomsk Polytechnic University within the Federal Target Program on research and development according to priority research fields of the Russian science and technology sector for 2014-2020.

#### References

- [1] Yole Development //www.yole.fr
- [2] Russian MEMS association // www.mems-russia.ru/
- [3] Sistema monitoringa napryazhennogo sostoyaniya zdaniy i konstruktsii. Institut tochnoi mekhaniki i vychislitel'noi tekhniki im. S A Lebedeva RAN - nauchno-issledovatel'skii institut v oblasti informatsionnykh tekhnologii, vychislitel'noi tekhniki i mikroelektroniki [Stress-strain state monitoring systems. Lebedev Institute of Precision Mechanics and Computer Engineering] // www.ipmce.ru/custom/sensornetworks/products/smbuilding/
- [4] Nesterenko T G, Koleda A N, Barbin E S, Uchaikin SV (2014) *IEEE Transactions on components, packaging, and manufacturing technology* **4**(10) 1598–1605
- [5] Koleda A N, Barbin E S, Nesterenko T G (2015) Three-component microelectromechanical accelerometer *22nd Saint Petersburg International Conference on Integrated Navigation Systems, ICINS 2015 – Proceedings* 338–342
- [6] Nesterenko T G, Barbin E S, Koleda A N, Arshinova A A (2015) Metrological performance of integrated multiple axis MEMS accelerometers under thermal effect *XXI IMEKO World Congress 2015*